JOC*Article*

Electrophilic Chemistry of Thia-PAHs: Stable Carbocations (NMR and DFT), S-Alkylated Onium Salts, Model Electrophilic Substitutions (Nitration and Bromination), and Mutagenicity Assay

Kenneth K. Laali,* Joong-Hyun Chun, and Takao Okazaki
Department of Chemistry, Kent State University, Kent, Ohio 44242

Subodh Kumar
Environmental Toxicology and Chemistry Laboratory, Great Lakes Center, State University of New York, College at Buffalo, Buffalo, New York 14222

Gabriela L. Borosky
Unidad de Matemática y Física, INFIQC, Facultad de Ciencias Químicas, Universidad Nacional de Córdoba, Ciudad Universitaria, Córdoba 5000, Argentina

Carol Swartz
Environmental Carcinogenesis Division, US Environmental Protection Agency, Research Triangle Park, North Carolina 27711

klaali@kent.edu

Received July 10, 2007

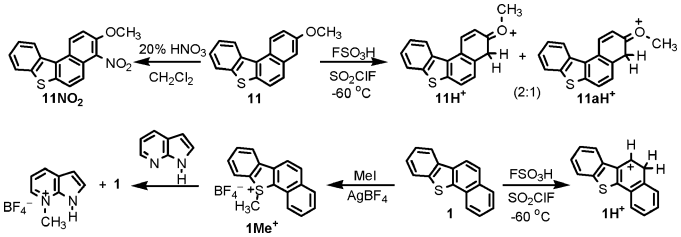

First examples of stable carbocations are reported from several classes of thia-PAHs with four fused rings, namely, benzo[*b*]naphtho[2,1-*d*]thiophene (**1**) and its 3-methoxy derivative (**2**), phenanthro[4,3-*b*]thiophene (**3**) and its 7-methoxy (**4**), 10-methoxy (**5**), and 9-methoxy (**6**) derivatives, phenanthro[3,4-*b*]thiophene (**7**) and its 7-methoxy (**8**) and 9-methoxy (**9**) derivatives, and 3-methoxybenzo[*b*]naphtha[1,2-*d*]thiophene (**11**). In several cases, the resulting carbocations were also studied by GIAO-DFT. Charge delocalization modes in the resulting carbocations were probed. A series of S-alkylated onium tetrafluoroborates, namely, **1Me**$^+$, **1Et**$^+$, **2Et**$^+$, and **7Me**$^+$ (from **1**, **2**, and **7**), **10Me**$^+$ and **10Et**$^+$ (from benzo[*b*]naphtha[1,2-*d*]thiophene **10**), **12Me**$^+$ and **12Et**$^+$ (from phenanthro[3,2-*b*][1]benzothiophene **12**), **13Me**$^+$ (from 3-methoxyphenanthro[3,2-*b*]benzothiophene **13**), **14Me**$^+$ (from phenanthro[4,3-*b*][1]-benzothiophene **14**), and **15Me**$^+$ (from 3-methoxyphenanthro[4,3-*b*][1]benzothiophene **15**), were synthesized. PAH-sulfonium salts **1Me**$^+$, **1Et**$^+$, **10Me**$^+$, **10Et**$^+$, **12Me**$^+$, and **14Me**$^+$ proved to be efficient akylating agents toward model nitrogen nucleophile receptors (imidazole and azaindole). Facile trans-alkylation to model nucleophiles (including guanine) is also supported by favorable reaction energies computed by DFT. Ring opening energies in thia-PAH-epoxides from **1**, **3**, and **7** and charge delocalization modes in the resulting carbocations were also evaluated. The four-ring-fused thia-PAHs **1**, **2**, **3**, **4**, **5**, **7**, **8**, and **11** are effectively nitrated under extremely mild conditions. Nitration regioselectivity corresponds closely to protonation under stable ion conditions. Bromination of **4** and **6** is also reported. Comparative mutagenicity assays (Ames test) were performed on **1** versus **1NO$_2$**, **5** versus **5NO$_2$**, and **11** versus **11NO$_2$**. Compound **5NO$_2$** was found to be a potent direct acting mutagen.

Introduction

Studies aimed at understanding the mechanism of activation of thia-PAHs (the sulfur analogues of PAHs) have been quite limited, despite their recognition as widely distributed environmental contaminants with mutagenic and carcinogenic activity.[1,2] Synthesis and bioassay of the four-ring-fused systems, namely,

* To whom correspondence should be addressed. E-mail: klaali@kent.edu. Fax: 330-6723816. Tel: 330-6722988.

(1) Jacob, J. *Sulfur Analogues of Polycyclic Aromatic Hydrocarbons*; Cambridge University Press: Cambridge, UK, 1990.

10.1021/jo701502y CCC: $37.00
Published on Web 10/02/2007

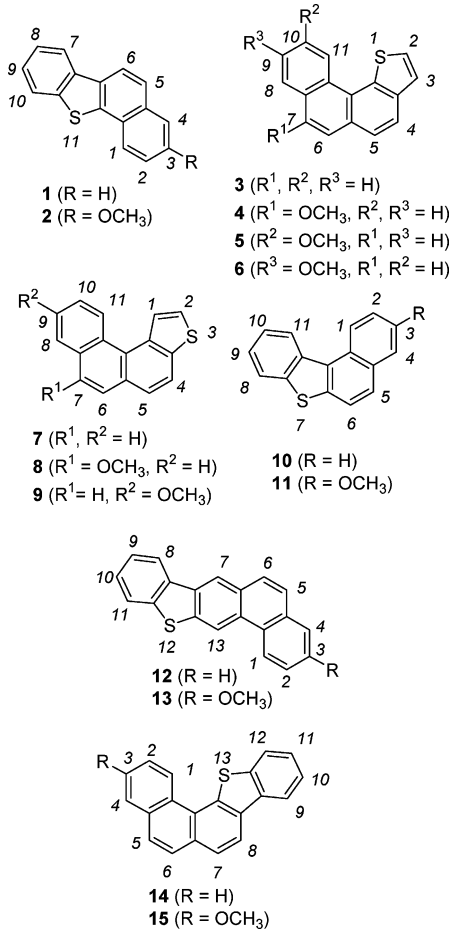

FIGURE 1. Studied thia-PAHs.

benzo[*b*]naphtho[2,1-*d*]thiophene **1**, phenanthro[4,3-*b*]thiophene **3**, and the isomeric phenanthro[3,4-*b*]thiophene **7**, have been reported (see Figure 1).[3−8]

Compound **1** can be viewed as a thia-chrysene with two bay regions. Its 1,2- and 3,4-dihydrodiols have been synthesized.[3,4] The metabolism of **1** was suggested to be in part via bay region diol epoxide and in part by sulfur activation (sulfoxide and sulfone formation). The 5-nitro derivative of **1** binds to DNA, and the structures of the metabolites indicated both ring oxidation and nitro reduction.[5] Compounds **3** and its isomer **7** can be viewed as the sulfur analogues of benzo[*c*]phenanthrene BcPh. Interestingly, whereas **3** (sulfur in the fjord region) is not mutagenic, **7** was reported to be as mutagenic as benzo[*a*]-pyrene (BaP).[8] Syntheses of the 6,7-dihydrodiol and 8,9-dihydrodiol of **3** and **7** were reported.[7,8] Among the five-ring-fused systems, phenanthro[3,2-*b*][1]benzothiophene **12** and phenanthro[4,3-*b*][1]benzothiophene **14** (in Figure 1) have been the subject of synthetic and bioassay study.[9−11] Compound **12**, which could be viewed as the sulfur analogue of dibenz[*a*,*h*]-anthracene DBA, is a strong carcinogen (more active than DBA).[9]

Synthesis of its 3,4-dihydrodiol was reported.[9] Metabolic activation by rodent liver microsomes produced the 3,4-dihydrodiol and the sulfoxide as major metabolites.[10] Compound **14** is a benzannulated analogue of **3** with a fjord region. Synthesis of its 3,4-dihydrodiol was reported.[11]

The majority of polyaromatic heterocyclic compounds studied for their potential as DNA intercalators are aza-PAHs, for which there are numerous literature reports, in particular on diazapyrenium,[12] phenanthridinium,[13−15] and benzo[*c*]phenanthridinium salts,[16] as analogues of ethidinium. Examples of sulfonium-based DNA intercalators do not appear to exist. Availability of the compounds listed in Figure 1 (parent systems and isomeric methoxy derivatives) provided the impetus for the present multifaceted investigation that combined stable carbocation generation with the synthesis of several S-alkylated onium salts, including a study of their transfer alkylation toward imidazole and azaindole as representative nitrogen nucleophile receptors. Using nitration (and bromination) as model electrophilic reactions, a number of new derivatives were synthesized. DFT was used to model epoxide ring opening in thia-PAHs, and mutagenicity tests (Ames assay) were performed on the nitro derivatives of **1**, **5**, and **11**.

Results and Discussion

(a) Stable Carbocations from Thia-PAHs 1 and 2 (Figure 2a,b, Chart S1, Table S1). Low-temperature protonation of **1** in FSO_3H/SO_2ClF gave $\mathbf{1H}^+$ by attack at C-5 (Figure 2a). This outcome agrees with DFT (Table S1) showing that, among all possible protonation sites, the carbocation derived from attack at C-5 has the lowest energy, with S-protonation computed to be significantly less favorable. For comparison, the NMR data for $\mathbf{1H}^+$ (a thia-arenium ion) and $\mathbf{1H_2}^{2+}$ (a sulfonium-arenium dication) were computed by GIAO-NMR (Figure 2b). The experimental NMR data (Figure 2b) correlate more closely with the GIAO for $\mathbf{1H}^+$. On this basis, significant involvement of $\mathbf{1H_2}^{2+}$ was ruled out, although limited equilibrium protonation at sulfur cannot be excluded. Charge delocalization in $\mathbf{1H}^+$ is primarily confined to the naphthalenium moiety. Whereas the NPA-derived changes in charges (Δq) agree with the NMR-derived charge map, it also places significant positive charge at sulfur (Figure 2b).

(2) Harvery, R. G. In *The Handbook of Environmental Chemistry*; Neilson, A. H., Ed.; Springer-Verlag: Berlin, 1998; Vol. 1, Part 1, and other related references cited therein.
(3) Kumar, S.; Kim, T.-Y. *J. Org. Chem.* **2000**, *65*, 3883−3884.
(4) Misra, B.; Amin, S. *Chem. Res. Toxicol.* **1990**, *3*, 93−97.
(5) King, L. C.; Kohan, M. J.; Brooks, L.; Nelson, G. B.; Ross, J. A.; Allison, J.; Adams, L.; Desai, D.; Amin, S.; Padgett, W.; Lambert, G. R.; Richard, A. M.; Nesnow, S. *Chem. Res. Toxicol.* **2001**, *14*, 661−671.
(6) Kumar, S.; Kumar, A.; Sikka, H. C. *Polycyclic Aromat. Compd.* **2004**, *24*, 527−536.
(7) Kumar, S.; Saravanan, S.; Reuben, P.; Kumar, A. *J. Heterocycl. Chem.* **2005**, *42*, 1345−1355.
(8) (a) Kumar, S.; Reuben, P. A.; Kumar, A. *Polycyclic Aromat. Compd.* **2004**, *24*, 289−295. (b) Pelroy, R. A.; Stewart, D. L.; Tominaga, Y.; Iwao, M.; Castle, R. N.; Lee, M. L. *Mutat. Res.* **1983**, *117*, 31−40.
(9) Kumar, S. *J. Chem. Soc., Perkin Trans. 1* **2001**, 1018−1023.
(10) Yuan, Z.-X.; Sikka, H. C.; Munir, S.; Kumar, A.; Muruganandam, A. V.; Kumar, S. *Chem. Res. Toxicol.* **2003**, *16*, 1581−1588.
(11) Kumar, S. *J. Org. Chem.* **2002**, *67*, 8842−8846.
(12) (a) Piantanida, I.; Palm, B. S.; Zinic, M.; Schneider, H.-J. *J. Chem. Soc., Perkin Trans. 2* **2001**, 1808−1816. (b) Palm, B. S.; Piantanida, I.; Zinic, M.; Schneider, H.-J. *J. Chem. Soc., Perkin Trans. 2* **2000**, 385−392. (c) Piantanida, I.; Tomisic, V.; Zinic, M. *J. Chem. Soc., Perkin Trans. 2* **2000**, 375−383. (d) Steiner-Biocic, I.; Glavas-Obrovac, L.; Karner, I.; Piantanida, I.; Zinic, M.; Pavelic, K.; Pavelic, J. *Anticancer Res.* **1996**, *16*, 3705−3708.
(13) Tumir, L.-M.; Piantanida, I.; Cindric, I. J.; Hrenar, T.; Meic, Z.; Zinic, M. *J. Phys. Org. Chem.* **2003**, *16*, 891−899.
(14) Huber, R.; Amann, N.; Wagenknecht, H.-A. *J. Org. Chem.* **2004**, *69*, 744−751.
(15) Ross, S. A.; Pitie, M.; Meunier, B. *J. Chem. Soc., Perkin Trans. 1* **2000**, 571−574.
(16) Nakanishi, T.; Suzuki, M.; Mashiba, A.; Ishikawa, K.; Yokotsuka, T. *J. Org. Chem.* **1998**, *63*, 4235−4239.

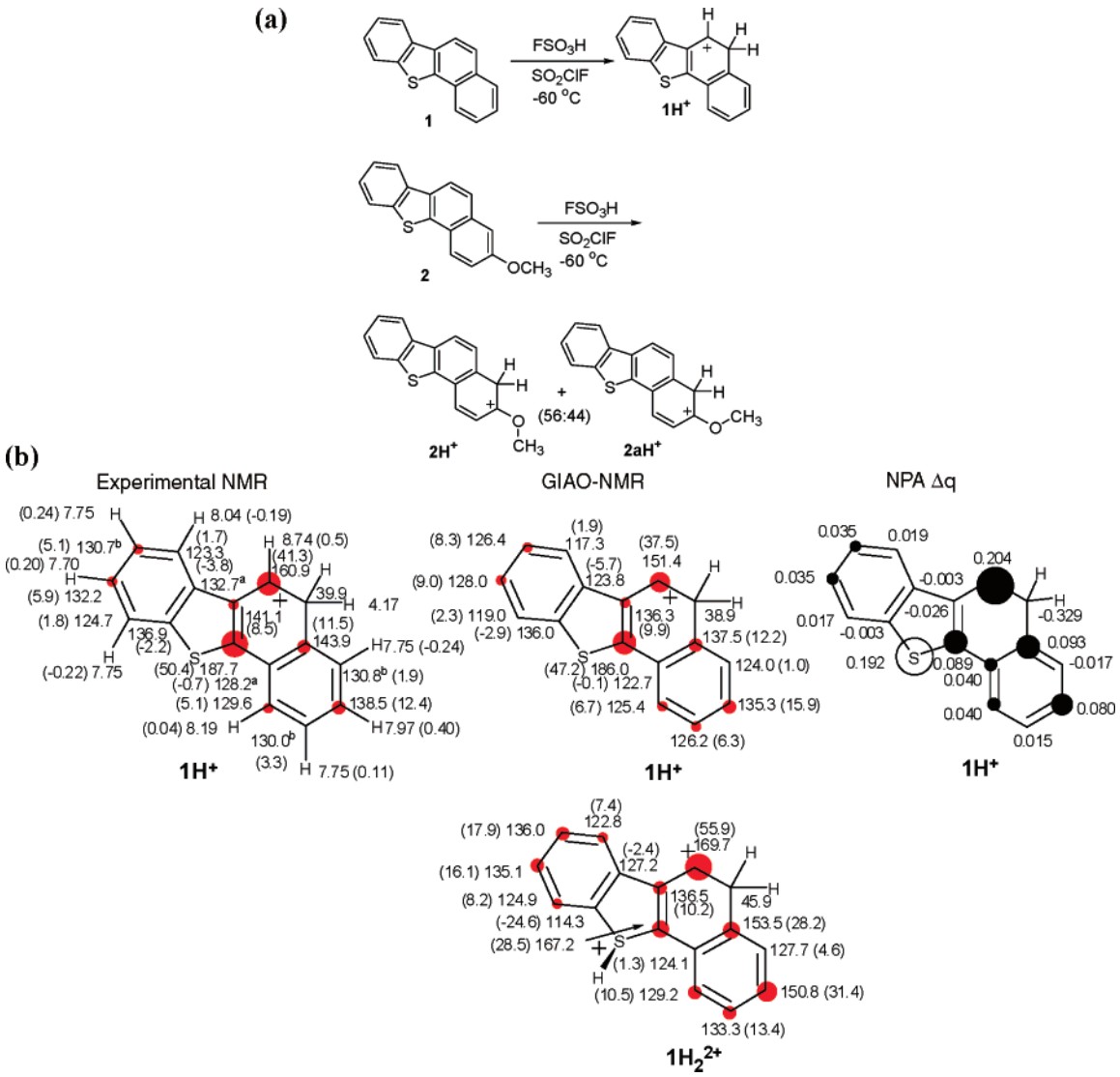

FIGURE 2. (a) Protonation of **1** and **2** in FSO_3H/SO_2ClF. (b) Experimental and GIAO/B3LYP/6-31G(d)-derived NMR chemical shifts for $\mathbf{1H}^+$ and $\mathbf{1H_2}^{2+}$, $\Delta\delta^{13}C$ values (in parentheses) relative to those for the parent **1** (red circles are roughly proportional to magnitude of $\Delta\delta^{13}C$ values, threshold 5 ppm; a and b designations refer to interchangeable assignments), and changes in the NPA-derived charges (Δq) for $\mathbf{1H}^+$ (dark circles are roughly proportional to C Δq and white circle to S Δq, threshold was set to 0.030).

Strong directive effect of the methoxy substituent becomes evident in low-temperature protonation of the 3-methoxy derivative **2** (Figure 2a), which on low-temperature reaction with FSO_3H/SO_2ClF gave $\mathbf{2H}^+$ and $\mathbf{2aH}^+$ (as two geometrical isomers) by attack at C-4 (in 56:44 ratio). The identity of each conformer was established via NOE experiments. NMR assignments of the two species (in particular those of the quaternary ring junction carbons) were aided by GIAO calculations (see Chart S1). Charge delocalization mode in $\mathbf{2H}^+$ and $\mathbf{2aH}^+$signify strong naphthalenium ion character in these carbocations.

(b) Stable Carbocations from Thia-PAHs 3, 4, 5, and 6 (Figure 3, Chart S2, Tables S1 and S2). Low-temperature protonation of **3** with FSO_3H/SO_2ClF led to the formation of $\mathbf{3H}^+$ as the sole carbocation (protonation at C-2) (Figure 3). This underlines the importance of benzylic delocalization as compared to α-sulfur stabilization (protonation at C-3). DFT concurs (Table S1), showing that the carbocation derived from protonation at C-2 is the most stable, with C-3 protonation computed to be 14 kcal/mol less favorable. Chart S2 provides a summary of the experimental NMR assignments for $\mathbf{3H}^+$ and its GIAO-derived data. The charge delocalization mode deduced based on magnitude of $\Delta\delta^{13}C$ is in good agreement with the NPA-derived charge pattern based on Δq (Chart S2), showing relatively extensive delocalization throughout the system with highest charge localization at C-3 in the five-membered ring. Directive effect of the methoxy group manifested itself in the protonation of the 7-methoxy derivative **4**, which gave a mixture of two carbocations $\mathbf{4H}^+$ (protonation at C-6; α to methoxy) and $\mathbf{4aH}^+$ (protonation at C-2; α to sulfur). At the onset, the carbocation ratio was 2:1 in favor of $\mathbf{4H}^+$, changing subsequently to 2:3. According to DFT, $\mathbf{4aH}^+$ is 4.9 kcal/mol more stable (Table S2). Variation in carbocation ratios in solution likely originates from variation in local overheating on contact with the superacid at low temperature.

Experimental and GIAO-derived NMR data for $\mathbf{4H}^+$ and $\mathbf{4aH}^+$ are summarized in Chart S2. Assignment of the relative geometry of the OMe group in $\mathbf{4H}^+$ was based on NOE. Positive charge in $\mathbf{4H}^+$ (a thia-carboxonium ion) is primarily localized at the carboxonium group and the benzannelated ring. In $\mathbf{4aH}^+$,

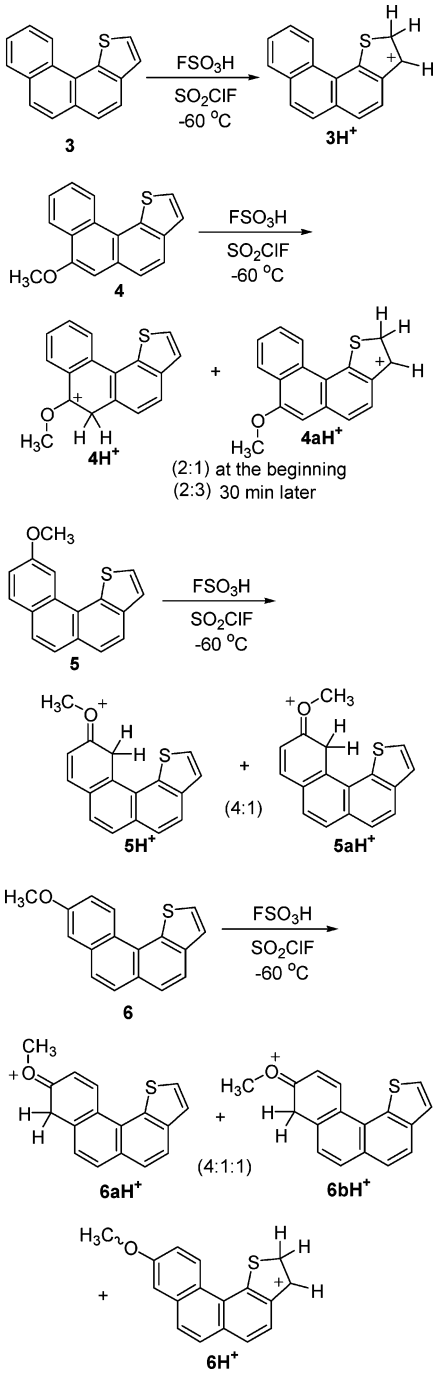

FIGURE 3. Protonation of **3**−**6** in FSO_3H/SO_2ClF.

positive charge is mainly localized at the five-membered ring with limited delocalization throughout the periphery.

An interesting outcome was observed in the low-temperature protonation of the 10-methoxy derivative **5** with FSO_3H/SO_2ClF, resulting in the formation of $\mathbf{5H}^+$ and $\mathbf{5aH}^+$, as two geometrical isomers (in 4:1 ratio) by protonation in the fjord region (at C-11). Relative assignments of the two conformers were established by NOE.

On the basis of the DFT, $\mathbf{5H}^+$ is 1.8 kcal/mol more stable than $\mathbf{5aH}^+$, and protonation at the other α-methoxy position (C-9) is 6.4 kcal/mol less favorable relative to $\mathbf{5aH}^+$. Fine-tuning of the experimental NMR assignments for $\mathbf{5H}^+$ and $\mathbf{5aH}^+$ (in particular with respect to ring junction carbons) was assisted by the GIAO-DFT data and results are gathered in Chart S2 for comparison.

Low-temperature protonation of the 9-methoxy derivative **6** with FSO_3H/SO_2ClF resulted in the formation of three carbocations, namely, $\mathbf{6H}^+$ (protonation at C-2), and $\mathbf{6aH}^+/\mathbf{6bH}^+$ (two geometrical isomers, formed by protonation at C-8; α to methoxy) in 1:4:1 ratio, respectively. Relative assignments for $\mathbf{6aH}^+/\mathbf{6bH}^+$ were derived from NOE, and GIAO trends were used as a guide to fine-tune the experimental NMR assignments (Chart S2).

(c) Stable Carbocations from Thia-PAHs 7, 8, and 9 (Figure 4a,b, Chart S3, Table S1). Low-temperature reaction of **7** with FSO_3H/SO_2ClF resulted in protonation at C-2 to give $\mathbf{7H}^+$ as the sole carbocation (Figure 4a). This outcome agrees with DFT, showing that, among all possible protonation sites, C-2 protonation was best, with C-5 protonation as the next best possibility, lying 4.4 kcal/mol higher (Table S1). Experimental and GIAO NMR data for $\mathbf{7H}^+$ are collected in Figure 4b for comparison. Whereas the $\Delta\delta^{13}$C-derived charge delocalization map indicates extensive delocalization throughout the thiarenium ion, highest charge localizations are at C-1, C-3a, and C-5. This agrees with the charge map derived via NPA-derived Δq values (Figure 4b).

Protonation regioselectivity observed in **7** changed entirely when methoxy substituents were introduced at C-7 (compound **8**) and at C-9 (compound **9**), whereby carbocation $\mathbf{8H}^+$ was generated from **8** as the sole carbocation by attack at C-6 (α to OMe), and $\mathbf{9H}^+$ and $\mathbf{9aH}^+$ were obtained from **9** as geometrical isomers (in 4:1 ratio), by protonation at C-9 (α to OMe) (Figure 4a). Experimental and GIAO NMR data for $\mathbf{8H}^+$ and for $\mathbf{9H}^+/\mathbf{9aH}^+$ are gathered in Chart S3 for cross comparison. Charge delocalization in $\mathbf{8H}^+$ is mainly confined to the carboxonium center and the benzannelated ring. Similarly, limited charge delocalization is noted in $\mathbf{9H}^+/\mathbf{9aH}^+$, with positive charge mainly localized in the methoxy-bearing ring and on one conjugated ring carbon.

(d) Protonation of Thia-PAH 11 (Figure 5, Chart S4). Whereas low-temperature reaction of parent **10** with FSO_3H/SO_2ClF resulted in poorly resolved spectra that could not be analyzed, the 3-methoxy derivative **11** gave relatively improved spectra showing the formation of $\mathbf{11H}^+/\mathbf{11aH}^+$ as geometrical isomers (in 2:1 ratio) (Figure 5), for which partial NMR assignments could be made (Chart S1). This outcome once again underscores the influence of the OMe substituents in directing electrophilic attack.

(e) Synthesis of Onium Salts by S-Alkylation (Figure 6, Chart S5). As mentioned in the Introduction, in the context of the present study and in order to further develop the electrophilic chemistry of thia-PAHs, we focused on synthesis and characterization of model sulfonium salts derived from compounds listed in Figure 1 and examined their potential as alkylating agents in model reactions. Whereas trialkyl(aryl)sulfonium salts are readily prepared by reaction with a variety of alkylating agents,[17a] initial studies aimed at developing suitable alkylating systems for thia-chrysene **1** proved to be unexpectedly challenging. Thus, attempted alkylation with EtOTf either without an added Lewis acid or in the presence of various promoters such as AgOTf, BF_3/Et_2O, and $Sc(OTf)_3$ at rt in CH_2Cl_2 or under

(17) (a) Olah, G. A.; Laali, K. K.; Wang, Q.; Prakash, G. K. S. *Onium Ions*; Wiley: New York, 1998; Chapter 4. (b) Olah, G. A.; Laali, K.K.; Wang, Q.; Prakash, G. K. S. *Onium Ions*; Wiley: New York, 1998; Chapter 7.

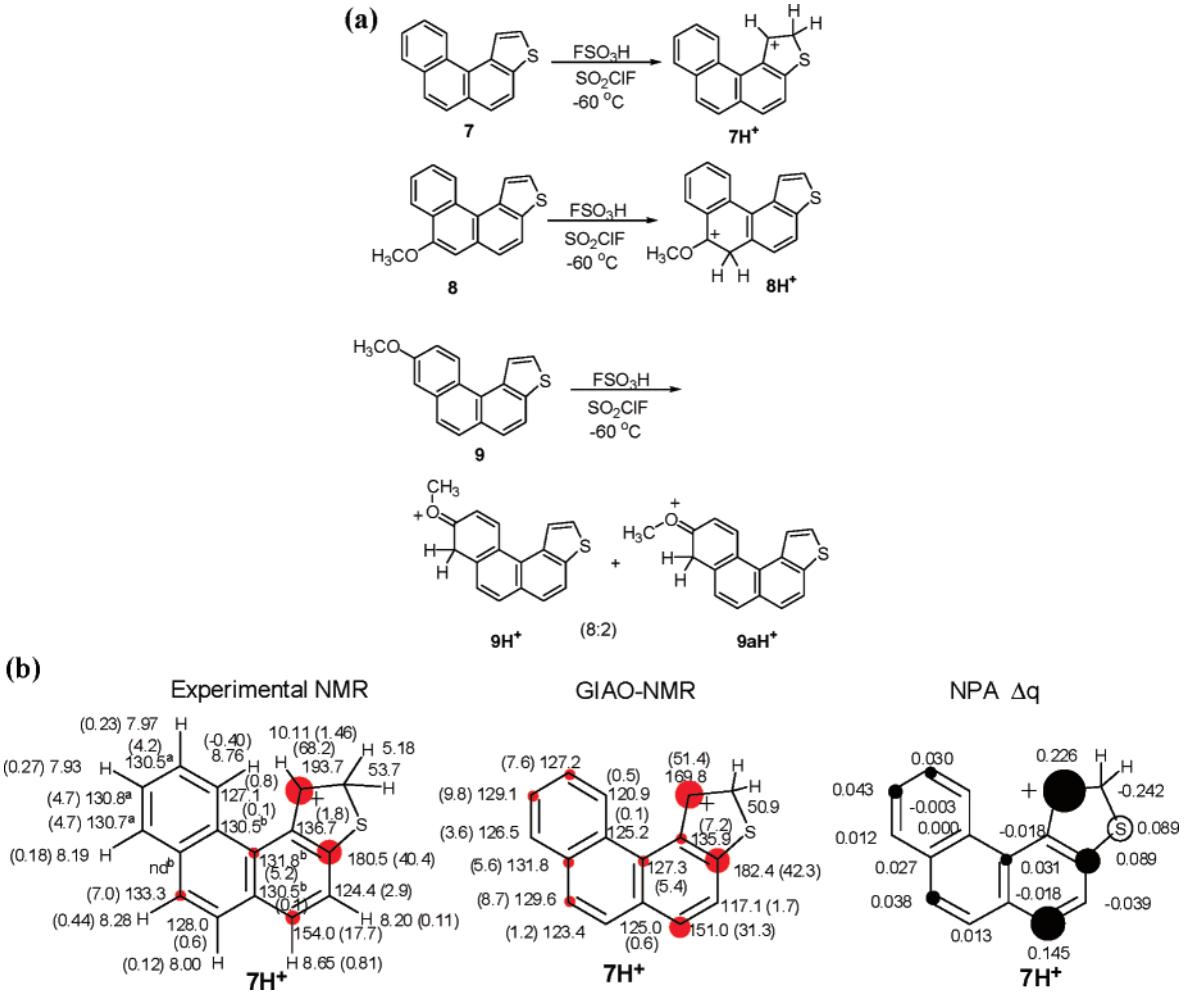

FIGURE 4. (a) Protonation of **7**−**9** in FSO_3H/SO_2ClF. (b) Experimental and GIAO/B3LYP/6-31G(d)-derived NMR chemical shifts for **7H**$^+$, and $\Delta\delta^{13}$C values (in parentheses) relative to those for the parent **7** (red circles are roughly proportional to magnitude of $\Delta\delta^{13}$C values, threshold 5 ppm; a and b designations refer to interchangeable assignments; nd = not detected), and changes in the NPA-derived charges (Δq) for **7H**$^+$ (dark circles are roughly proportional to C Δq and white circle to S Δq, threshold was set to 0.030).

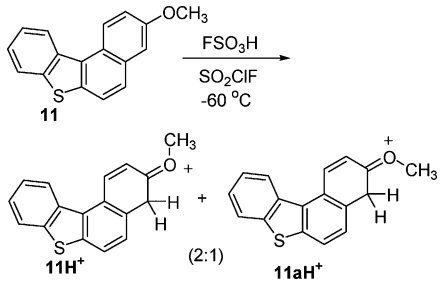

FIGURE 5. Protonation of **11**.

reflux in 1,2-dichloroethane (DCE) proved unsuccessful, with ^{1}H NMR monitoring of the reactions indicating no conversion!

Similar attempts using EtI/AgOTf in DCE under reflux also proved unsuccessful. Fortunately, S-alkylation occurred when AgOTf was replaced with $AgBF_4$. The alkylating system RI/$AgBF_4$/DCE was therefore selected for the entire study. In their early work on synthesis of S-alkylated thiophenium salts, Acheson and Harrison[18] experienced the same difficulties and selected the RI/$AgBF_4$/DCE system for their study.

(18) Acheson, R. M.; Harrison, D.R. *J. Chem. Soc. (C)* **1970**, 1764−1784.

Six examples of four-ring-fused sulfonium salts, namely, **1Me**$^+$, **1Et**$^+$, **2Et**$^+$, **7Me**$^+$, **10Me**$^+$, and **10Et**$^+$, and six examples of five-ring-fused sulfonium salts, namely, **12Me**$^+$, **12Et**$^+$, **13Me**$^+$, **14Me**$^+$, **14Et**$^+$, and **15Me**$^+$, were synthesized via this route (Figure 6).

Specific NMR assignments were made for the sulfonium ions **1Me**$^+$, **1Et**$^+$, **10Me**$^+$, **12Me**$^+$, and **12Et**$^+$ with the aid of 2D NMR techniques (Chart S5) (for regular NMR data of all sulfonium salts, see Experimental Section). The sulfonium cations **1Me**$^+$, **1Et**$^+$, and **12Me**$^+$ were also calculated by GIAO NMR for comparison and as an aid to fine-tuning the experiment-derived assignments (included in Chart S5). The sulfonium salts were also studied by electrospray-MS (Experimental Section).

In contrast to their carbocations, the sulfonium salts exhibit limited charge delocalization into the aromatic system. A notable feature in the ^{1}H NMR spectra of the ethylated salts is the diastereotopic nature of $-SCH_2CH_3$ protons giving rise to a pair of doublets. Figure 7 shows the DFT-optimized structure of **1Et**$^+$. Pyramidalization at sulfur creates an asymmetric center. Figure S1 depicts the computed sulfur orbitals by NBO analysis, which infer sp^3 hybridization at sulfur.

Sulfonium salts **14Me**$^+$, **14Et**$^+$, and **15Me**$^+$ represent novel examples of S-alkylation in the crowded fjord region.

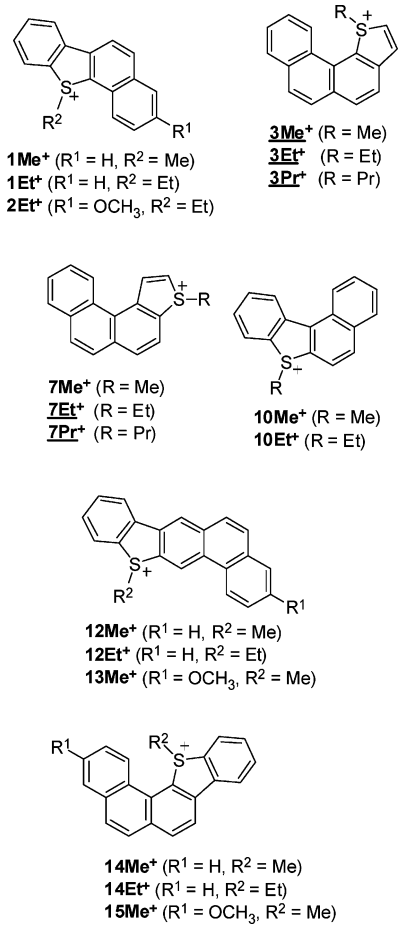

FIGURE 6. Synthesis of S-alkylated onium salts from thia-PAHs (all sulfonium salts listed were synthesized, except those that are underlined, which were only studied computationally).

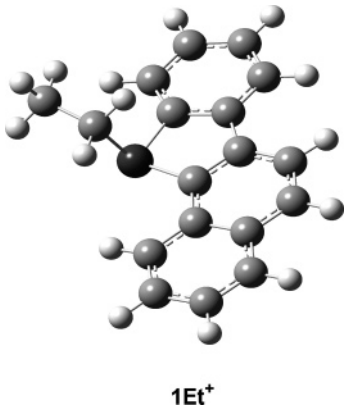

1Et$^+$

FIGURE 7. Optimized structure of **1Et**$^+$ by B3LYP/6-31G(d).

The NMR spectrum of **1Me**$^+$ salt dissolved in FSO_3H/SO_2ClF indicated only small variations relative to $CDCl_3$ and was not indicative of ring protonation to form a sulfonium-arenium dication. Attempts to generate a dication by dissolving **1Me**$^+$ salt in higher acidity superacid FSO_3H/SbF_5(1:1)/SO_2ClF led to side reactions and degradation of the onium salt.

(f) Transfer Alkylation to Model Nitrogen Nucleophile Receptors (Scheme 1, Table S3). Facile alkylation of imidazole was observed on mixing with sulfonium salts **1Me**$^+$ and **1Et**$^+$ at rt in $CDCl_3$, as evidenced by ^{1}H NMR monitoring experiments showing rapid decrease in the S-*Me*$^+$ and S-*Et*$^+$ signals concomitant with the appearance of the imidazolium N-*Me*$^+$ and N-*Et*$^+$ signals (Scheme 1). Similar transalkylation reactions were performed with **1Me**$^+$, **1Et**$^+$, **10Me**$^+$, **10Et**$^+$, **12Me**$^+$, and **14Me**$^+$ salts toward azaindole as model, in CD_3CN or $CDCl_3$ as solvents. These reactions indicated facile transalkylation (usually complete within 30 min), with the formation of N-alkylated azaindole (see Scheme 1).

As a guide, the reaction energies for alkyl transfer to nitrogen nucleophiles (imidazole, azaindole, and adenine) were computed by DFT (Table S3) for the sulfonium salts **1Me**$^+$, **3Me**$^+$, **3Et**$^+$, **3Pr**$^+$, **7Me**$^+$, **7Et**$^+$, **7Pr**$^+$, **10Me**$^+$, **12Me**$^+$, and **14Me**$^+$. Reactions were found to be highly favorable, with those for adenine alkylation being the most favored.

Our model studies indicate that thia-PAHs are promising candidates for DNA intercalation/alkylation studies.

(g) Model Electrophilic Aromatic Substitution Reactions (Scheme 2). In order to compare the regioselectivities observed in carbocation generation under stable ion conditions with those resulting from conventional electrophilic aromatic substitutions, protic nitration of thia-PAHs **1**−**5** as well as **8** and **11** were studied. In addition, bromination of **4** and **6** was also examined. Nitration of parent thia-chrysene **1** using mixed acid and formation of the 5-nitro derivative and its bioassay was reported by King et al.[5]In our hands, compound **1** was cleanly nitrated under extremely mild conditions (20% aqueous nitric acid), without the need to use mixed acids, to give **5NO$_2$**. Common regioselectivity (attack at C-5) was, therefore, established in protonation and nitration of **1**, in concert with DFT. Similar mild nitration of the 3-methoxy derivative **2** gave a 60:40 mixture of **2NO$_2$** (attack at C-5) and **2aNO$_2$** (attack at C-4, α to OMe).

Directive effect of the methoxy substituent is further manifested in comparative nitrations of compounds **3**, **4**, and **5**. Mild nitration of parent **3** gave two mono-nitrated products, namely, **3NO$_2$** and **3aNO$_2$**, in 3:1 ratio. The latter matches the regioselectivity of the carbocation (**3H**$^+$), whereas the former (attack at C-7) corresponds to the next best intermediate (by DFT) lying 6.5 kcal/mol higher (see Table S1). Remarkably, nitration of the 7-methoxy derivative **4** could be effected in 10% aqueous nitric acid to give **4NO$_2$** in good yield (substitution at C-6). Under stable ion conditions, two carbocations (protonation at C-6 and at C-2) were observed.

Nitration of the 10-methoxy derivative **5** gave **5NO$_2$** (nitration at C-9), illustrating again the directive influence of the OMe group. As discussed earlier, protonation of **5** occurred at C-11 (fjord region), which based on DFT was preferred over C-9 protonation by 6.4 kcal/mol (Table S2). In the parent system **3**, this energy difference decreased to 5.2 kcal/mol (Table S1). Preferential nitration at C-11 likely originates from differences in steric demand for nitration versus protonation in the congested fjord region.

Mild nitration of **8** resulted in the formation of **8NO$_2$** (attack at C-7), and nitration of **11** gave **11NO$_2$** (attack at C-4), both cases representing common regioselectivities in protonation and nitration.

Finally, bromination of **4** (with NBS) gave **4Br** by substitution at C-2. This regioselectivity matches with the carbocation **4aH**$^+$ under stable ion conditions. Bromination of the 9-methoxy derivative **6** gave **6Br** as the major product, together with a dibrominated product **6Br$_2$** (in 5:1 ratio, respectively). Bromination regioselectivity in **6Br** corresponds to carbocations **6aH**$^+$/**6bH**$^+$ formed under stable ion conditions.

SCHEME 1. Facile Transfer Alkylation to Model Nitrogen Nucleophiles

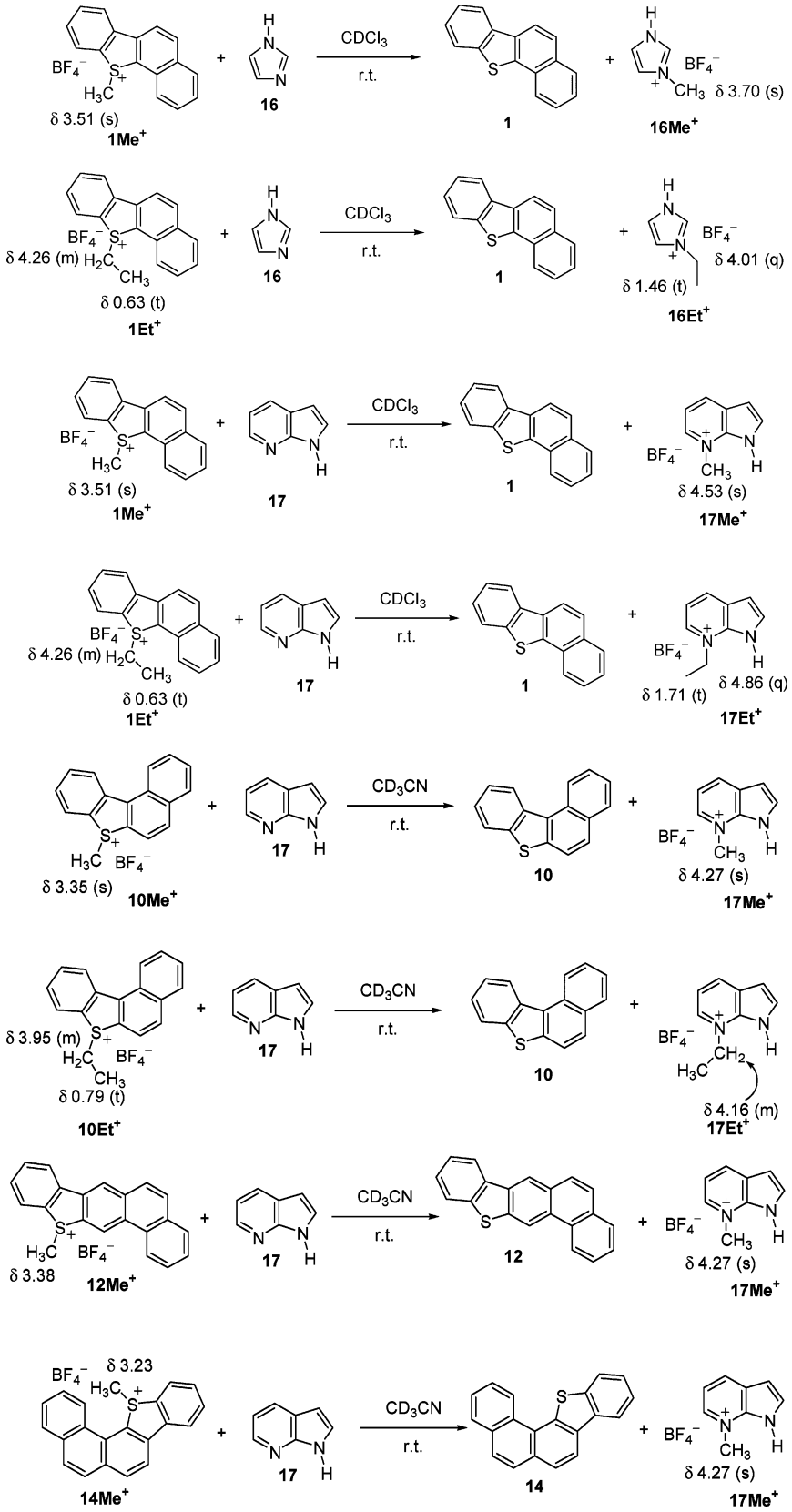

The observed differing regioselectivities in alkylation, taking place at sulfur, versus protonation and nitration reactions, which in agreement with DFT occurred at ring positions, may be rationalized considering the nature of the electrophiles involved. Steric demand of a polarized complex formed via RI/$AgBF_4$ is significantly larger as compared to protonation and nitration electrophiles. S-Alkylation is likely an S_N2-type displacement process assisted by the counterion (RI/$AgBF_4$ was effective but

SCHEME 2. Model Nitration and Bromination Reactions

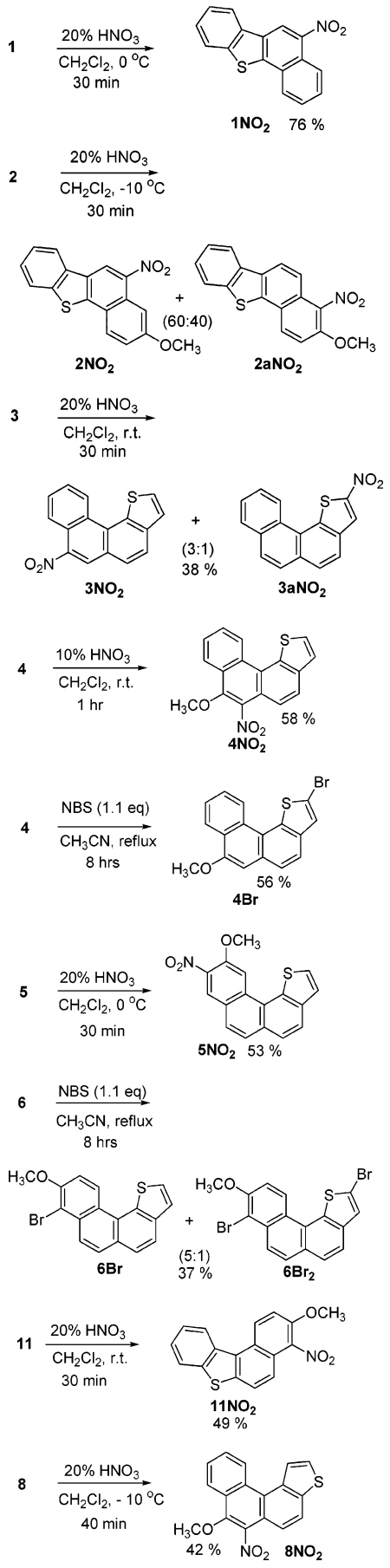

RI/AgOTf did not work!) and involves coupling of a soft nucleophile with a polarized complex.

(h) Modeling Thia-PAH Epoxide Ring Opening by DFT (Schemes S1 and S2, Chart S6). As highlighted in the Introduction, metabolism of **1** was suggested to be in part via bay region diol epoxide and in part by sulfur activation.[3,4] The diol epoxides **1a** and **1b** and their ring opening energies to form benzylic carbocations $\mathbf{1a}^+$ and $\mathbf{1b}^+$ were computed by DFT. As previously observed for aza-PAH epoxides,[19] ring opening of the protonated epoxides via thia-PAHs also occurred via barrierless processes. On the basis of DFT, formation of carbocation $\mathbf{1b}^+$ is 6 kcal/mol more favorable relative to $\mathbf{1a}^+$ (Scheme S1). This focuses attention on the possibility that oxidation at 7,8- and 9,10-positions may have biological significance and calls for synthesis and mutagenicity assay of their dihydrodiols. The NPA-derived changes in charges (Δq) (**1a** → $\mathbf{1a}^+$ and **1b** → $\mathbf{1b}^+$) are illustrated in Chart S6 for comparison. The Δq pattern for the energetically more favored $\mathbf{1b}^+$ implies that the carbocation resulting from 7,8-epoxide ring opening is mainly a carbosulfonium ion[17b] (positive charge resides mainly at sulfur and at C-10a).

Focusing on the fjord region, thia-PAHs **3** (not mutagenic), and **7** (mutagenic) (see Introduction), the epoxide ring opening energies were computed by DFT, taking into account all possible epoxides (Scheme S2). For comparison, charge delocalization pathways in the resulting carbocations were also deduced based on magnitude of Δq (Chart S6).

Carbocation formed via the 8,9-epoxide ring opening (**3d** → $\mathbf{3d}^+$) has the lowest energy. Ring opening energies for the K-region epoxide **3b** and the fjord region epoxide **3e** are nearly identical (∼2 kcal/mol above **3d**). That of 6,7-epoxide **3c** (whose dihydrodiol has been synthesized)[7,8a] is an additional 2 kcal/mol higher. Among various epoxides derived from **7**, ring opening of **7b** (generating $\mathbf{7b}^+$) is most favorable. Comparing the K-region epoxide ring opening energies between **3b** and **7b**, it can be seen that **7b** → $\mathbf{7b}^+$ is 4 kcal/mol more favorable than **3b** → $\mathbf{3b}^+$. This is interesting in light of the reported mutagenicity of **7**. As for the computed Δq maps (Chart S6), and focusing on the most favored ring openings $\mathbf{3d}^+$ and $\mathbf{7b}^+$, it can be deduced that positive charge in the former is mainly localized on the C/D rings, whereas $\mathbf{7b}^+$ implies a much more delocalized carbocation.

(i) Comparative Mutagenicity Assay on Selected Nitro Derivatives (Table 1). The mono-nitro derivatives **1NO2**, **5NO2**, and **11NO2** (see section g) and their precursors (**1**, **5**, and **11**) were subjected to mutagenicity assay by the Ames test. Among the precursors, compound **5** is most active (it is moderately potent with metabolic activation). Influence of nitration on mutagenic activity can be seen in comparing the nitro derivatives with their respective precursors. Nitration of **11** (→ **11NO2**) had little or no bioactivity enhancing effect. Nitration of **1** (→ **1NO2**) increased its mutagenic activity to some extent. Nitration of **5**, on the other hand, resulted in the formation of an extremely powerful direct acting mutagen. Given the extremely mild conditions under which the nitro derivatives are formed (see section g and experimental procedure in Supporting Information) and the proven presence of thia-PAHs in the environment, direct formation of the nitro derivatives in the environment appears quite feasible and could pose a health hazard.

(19) (a) Borosky, G. L.; Laali, K. K. *Chem. Res. Toxicol.* **2005**, *18*, 1876−1886. (b) Borosky, G. L.; Laali, K. K. *Org. Biomol. Chem.* **2005**, *3*, 1180−1188.

TABLE 1. Mutagenicity Assay by the Ames Test

sample	average potency (rev/μg)	average potency (rev/nmol)
1	29	7
1NO$_2$	281	78
1NO$_2$ with S9	268	75
5	116	31
5NO$_2$	5069	1566
5NO$_2$ with S9	198	61
11	0	0
11NO$_2$	0	0
11NO$_2$ with S9	20.5	6

Summary

In the context of the present multifaceted study aimed at developing the electrophilic chemistry of thia-PAHs, a series of novel carbocations were generated from four-ring-fused thia-PAHs and their regioisomeric methoxy derivatives. Regioselectivity issues and charge delocalization modes were addressed by NMR and by DFT studies. In view of the potential importance of hetero-PAHs and their onium salts as DNA intercalators and alkylating agents, a series of novel S-alkylated salts were synthesized and their potential as powerful alkylating agents toward nitrogen nucleophiles were demonstrated in model studies. To gain insight into structure/activity relationships, DFT was used to model epoxide ring opening reactions with the thia analogues of chrysene and benzo[*c*]phenanthrene and to examine their charge delocalization pathways as a function of epoxidation site and thia-PAH structure. Using nitration as model electrophilic substitution reactions, a series of nitro derivatives of thia-PAHs were synthesized under extremely mild conditions. Mutagenicity assays in representative cases demonstrated variable bioactivity, with one example (**5NO$_2$**) for generation of a potent direct acting mutagen.

Experimental Section

Synthesis of Onium Tetrafluoroborate Salts by S-Alkylation (For a Typical Alkylation Procedure, See Supporting Information): 1Me$^+$BF$_4^-$ was obtained as a beige solid (contained traces of unreacted **1** by ^{1}H NMR); yield, 2.8 mg (42%); ^{1}H NMR (400 MHz, $CDCl_3$) δ 8.58 (d, J = 8.0 Hz, 1H), 8.33 (d, J = 8.4 Hz, 1H), 8.19 (d, J = 8.0 Hz, 1H), 8.14 (d, J = 8.4 Hz, 1H), 8.08 (d, J = 8.4 Hz, 1H), 8.06 (d, J = 8.4 Hz, 1H), 7.87 (m, 1H), 7.83 (m, 1H), 7.74 (m, 2H), 3.51 (s, 3H); ^{13}C NMR (101 MHz, $CDCl_3$) δ 135.6 (CH), 134.2 (CH), 131.7 (CH), 131.0 (CH), 130.0 (CH), 129.2 (CH), 129.0 (CH), 124.2 (CH), 122.8 (CH), 119.7 (CH), 35.1 (CH_3); ES-MS (ESI+) *m*/*z* 247.9 [**1Me**$^+$], 584.1 [**1Me**$^+$]$_2$[BF_4^-], 920.2 [**1Me**$^+$]$_3$[BF_4^-]$_2$.

1Et$^+$BF$_4^-$: obtained as a beige solid (^{1}H NMR showed ca. 30% unreacted **1**); yield, 3.9 mg (29%); ^{1}H NMR (400 MHz, $CDCl_3$) δ 8.48 (d, J = 8 Hz, 1H), 8.31 (d, J = 8.4 Hz, 1H), 8.16 (d, J = 8.0 Hz, 1H), 8.13 (d, J = 8.4 Hz, 1H), 8.06 (d, J = 8.0 Hz, 1H), 8.04 (d, J = 8.0 Hz, 1H), 7.87 (m, 1H), 7.82 (m, 1H), 7.74 (m, 1H), 7.71 (m, 1H), 4.38 (m, 1H), 4.14 (m, 1H), 0.64 (t, J = 7.2 Hz, 3H); ^{13}C NMR (101 MHz, $CDCl_3$) δ 140.8 (C), 140.2 (C), 135.5 (CH), 134.1 (CH), 133.9 (C), 131.5 (CH), 130.9 (CH), 129.9 (CH), 129.2 (CH), 129.0 (CH), 128.9 (C), 127.2 (C),123.8 (CH), 122.9 (CH), 122.2 (C), 119.5 (CH), 44.5 (CH_2), 6.5 (CH_3); ES-MS (ESI+) *m*/*z* 262.7 [**1Et**$^+$]; MS/MS *m*/*z* 262.7 → 234.6 (**1Et**$^+$-C_2H_4).

2Et$^+$BF$_4^-$: ^{1}H NMR (400 MHz, $CDCl_3$) δ 8.46 (d, J = 8.0 Hz, 1H), 8.16 (d, J = 8.0 Hz, 1H), 8.06 (d, J = 8.0 Hz, 1H), 8.02 (d, J = 8.0 Hz, 1H), 7.96 (d, J = 8.0 Hz, 1H), 7.84 (t, J = 8.0 Hz, 1H), 7.71 (t, J = 8.0 Hz, 1H), 7.46 (d, J = 8.0 Hz, 1H), 7.33 (d, J = 2.4 Hz, 1H), 4.35 (m, 1H), 4.11 (m, 1H), 3.97 (s, 3H), 0.64 (t, J = 7.2 Hz, 3H); ES-MS (ESI+) *m*/*z* 293.2 [**2Et**$^+$]; MS/MS *m*/*z* 293.2 → 265.3 (**2Et**$^+$-C_2H_4).

7Me$^+$BF$_4^-$: ^{1}H NMR (400 MHz, acetone-d_6) δ 8.87 (d, J = 8.8 Hz, 1H), 8.50 (d, J = 8.4 Hz, 1H), 8.45 (d, J = 8.4 Hz, 1H), 8.40 (d, J = 8.0 Hz, 1H), 8.30 (d, J = 8.0 Hz, 1H), 8.16 (dd, J = 8.0, 1.2 Hz, 1H), 8.05 (d, J = 8.0 Hz, 1H), 8.03 (d, J = 8.0 Hz, 1H), 8.02−7.95 (m, 2H), 7.90−7.85 (m, 2H); ^{1}H NMR (400 MHz, $CDCl_3$) δ 8.83 (d, J = 8.0 Hz, 1H), 8.31 (d, J = 8.0 Hz, 1H), 8.10−7.90 (m, 8H), 3.41 (s, 3H);); ES-MS (ESI+) *m*/*z* 249.2 [**7Me**$^+$]; MS/MS *m*/*z* 249.2 → 234.0 (**7Me**$^+$-CH_3).

10Me$^+$BF$_4^-$: obtained as white solid (^{1}H NMR showed traces of unreacted **1**); yield, 5.2 mg (52%); ^{1}H NMR (400 MHz, CD_3CN) δ 8.99 (d, J = 8.4 Hz, 1H), 8.91 (d, J = 8.0 Hz, 1H), 8.33 (d, J = 8.0 Hz, 1H), 8.30 (d, J = 8.8 Hz, 1H), 8.21 (d, J = 8.4 Hz, 1H), 8.16 (d, J = 8.8 Hz, 1H), 8.02 (m, 1H), 7.92 (1H, m), 7.86 (1H, m), 7.84 (1H, m), 3.36 (s, 3H); ^{13}C NMR (101 MHz, CD_3CN) δ 141.3 (C), 136.8 (3C), 135.1 (CH), 133.5 (CH), 131.9 (C), 131.2 (CH), 131.0 (CH), 130.5 (CH), 130.2 (CH), 130.0 (C), 129.0 (CH), 128.5 (CH), 125.1 (CH), 122.2 (CH), 34.8 (CH_3); ES-MS (ESI+) *m*/*z* 248.6 [**10Me**$^+$].

10Et$^+$BF$_4^-$: obtained as brown solid (^{1}H NMR showed ca. 40% unreacted **10**); yield, 7.8 mg (crude, *approximately* 60%); ^{1}H NMR (400 MHz, CD_3CN) δ 8.96 (d, J = 8.8 Hz, 1H), 8.89 (d, J = 7.6 Hz, 1H), 8.28 (d, J = 9.2 Hz, 1H), 8.25 (d, J = 8.8 Hz, 1H), 8.19 (d, J = 8.0 Hz, 1H), 8.08 (d, J = 8.8 Hz, 1H), 8.01 (t, J = 7.6 Hz, 1H), 7.91 (t, J = 6.8 Hz, 1H), 7.87 (t, J = 8.0 Hz, 1H), 7.81 (t, J = 7.6 Hz, 1H), 3.95 (m, 2H), 0.79 (t, J = 7.2 Hz, 3H); ES-MS (ESI+) *m*/*z* 263.1 [**10Et**$^+$], 263.1 → 235.1 (**10Et**$^+$-C_2H_4).

12Me$^+$BF$_4^-$: obtained as white solid (^{1}H NMR showed traces of unreacted **12**); yield, 12.7 mg (54%); ^{1}H NMR (400 MHz, CD_3CN) δ 9.60 (s, 1H), 8.78 (s, 1H), 8.76 (d, J = 8.0 Hz, 1H), 8.37 (d, J = 8.0 Hz, 1H), 8.24 (d, J = 8.2 Hz, 1H), 8.08 (d, J = 8.8 Hz, 1H), 8.06 (d, J = 8.0 Hz, 1H), 8.01 (d, J = 8.8 Hz, 1H), 7.96 (m, 1H), 7.86 (m, 1H), 7.83 (m, 1H), 7.79 (m, 2H), 3.40 (s, 3H); ^{13}C NMR (101 MHz, CD_3CN) δ 140.1 (C), 136.8 (C), 135.9 (C), 135.1 (CH), 133.4 (C), 132.2 (CH), 132.0 (CH), 130.3 (C), 130.0 (CH), 129.5 (CH), 129.1 (CH), 128.6 (CH), 127.4 (CH), 125.2 (CH), 124.9 (CH), 124.7 (CH), 123.9 (CH), 35.8 (CH_3); ES-MS (ESI+) *m*/*z* 299.1 [**12Me**$^+$], 685.2 [**12Me**$^+$]$_2$[BF_4^-]; MS/MS *m*/*z* 299.1 → 284.1 (methyl loss).

12Et$^+$BF$_4^-$: obtained as white solid (^{1}H NMR showed ca. 10% unreacted **12**); yield, 5.7 mg (53%); ^{1}H NMR (400 MHz, CD_3CN) δ 9.43 (s, 1H), 8.70 (s, 1H), 8.71 (d, J = 8.4 Hz, 1H), 8.31 (d, J = 8.0 Hz, 1H), 8.15 (d, J = 8.0 Hz, 1H), 8.03 (d, J = 8.8 Hz, 1H), 7.96 (d, J = 8.8 Hz, 1H), 8.00 (d, J = 8.0 Hz, 2H), 7.94 (m, 1H), 7.81 (m, 1H), 7.79 (m, 1H), 7.73 (m, 1H), 3.96 (m, 1H), 3.91 (m, 1H), 0.84 (t, J = 7.0 Hz, 3H); ^{13}C NMR (101 MHz, CD_3CN) δ 141.2 (C), 137.6 (C), 135.9 (C), 135.2 (CH), 133.4 (C), 132.1 (CH), 132.0 (CH), 130.2 (C), 129.9 (CH), 129.4 (CH), 129.1 (CH), 129.0 (CH), 127.4 (CH), 125.1 (CH), 125.0 (CH), 124.7 (CH), 123.9 (CH), 46.5 (CH_2), 7.3 (CH_3); ES-MS (ESI+) *m*/*z* 312.5 [**12Et**$^+$].

13Me$^+$BF$_4^-$: obtained as beige solid (^{1}H NMR showed ca. 50% unreacted **13**); yield, 3.2 mg (crude, *approximately* 50%); ^{1}H NMR (400 MHz, CD_3CN) δ 9.43 (s, 1H), 8.72 (s, 1H), 8.63 (d, J = 9.2 Hz, 1H), 8.35−8.20 (m, 2H), 8.00−7.95 (m, 3H), 7.77 (t, J = 7.8 Hz, 1H), 7.49 (d, J = 2.4 Hz, 1H), 7.45 (dd, J = 9.2, 2.4 Hz, 1H), 3.98 (s, 3H), 3.38 (s, 3H); ES-MS (ESI+) *m*/*z* 329.2 [**13Me**$^+$], 745.2 [**13Me**$^+$]$_2$[BF_4^-]; MS/MS *m*/*z* 329 → 314.2 (methyl loss), 745.2 → 329.1 [**13Me**$^+$], 314.1 [**13Me**$^+$-CH_3].

14Me$^+$BF$_4^-$: obtained as brown solid (^{1}H NMR showed ca. 30% unreacted **14**); yield, 10.4 mg (crude, *approximately* 69%); ^{1}H NMR (400 MHz, CD_3CN) δ 8.74 (d, J = 8.4 Hz, 1H), 8.36 (d, J = 8.4 Hz, 1H), 8.32 (d, J = 8.4 Hz, 1H), 8.29 (d, J = 8.4 Hz, 1H), 8.23 (d, J = 8.0 Hz, 1H), 8.11 (d, J = 8.0 Hz, 1H), 7.98 (d, J = 8.8 Hz, 1H), 7.92 (d, J = 8.8 Hz, 1H), 7.95−7.75 (m, 4H), 3.18 (s, 3H); ^{1}H NMR (400 MHz, $CDCl_3$) δ 9.08 (d, J = 8.4 Hz, 1H), 8.64 (d, J = 8.0 Hz, 1H), 8.36 (d, J = 8.4 Hz, 1H), 8.27 (d, J = 8.4 Hz, 1H), 8.18 (d, J = 8.0 Hz, 1H), 8.10 (t, J = 8.4 Hz, 1H), 8.03 (d, J = 8.0 Hz, 1H), 7.93 (d, J = 8.8 Hz, 1H), 7.85−7.81 (m, 3H),

7.75 (t, J = 8.0 Hz, 1H), 3.39 (s, 3H); ES-MS (ESI+) m/z 298.9 [**14Me**$^+$], 685.0 [**14Me**$^+$]$_2$[BF_4^-]; MS/MS m/z 298.9 → 283.9 (methyl loss), m/z 685 → 583.0, 298.9, and 283.9.

14Et$^+$BF$_4^-$: ^{1}H NMR (400 MHz, CD_3CN) δ 8.88 (d, J = 8.4 Hz, 1H), 8.44 (d, J = 8.4 Hz, 1H), 8.40 (d, J = 8.4 Hz, 1H), 8.36 (d, J = 8.0 Hz, 1H), 8.23 (d, J = 8.0 Hz, 1H), 8.14 (d, J = 8.0 Hz, 1H), 8.02 (d, J = 8.8 Hz, 1H), 8.00−7.80 (m, 5H), 4.01 (m, 1H), 3.80 (m, 1H), 0.50 (t, J = 7.0 Hz, 3H); ES-MS (ESI+) m/z 312.3 [**14Et**$^+$]; MS/MS m/z 312.3 → 284.2.

15Me$^+$BF$_4^-$: obtained as light-brown solid (^{1}H NMR showed ca. 40% unreacted **15**); yield, 3.8 mg (crude, *approximately* 60%); ^{1}H NMR (400 MHz, CD_3CN) δ 8.62 (d, J = 9.2 Hz, 1H), 8.34 (d, J = 8.4 Hz, 1H), 8.31 (d, J = 7.6 Hz, 1H), 8.28 (d, J = 8.4 Hz, 1H), 8.24 (d, J = 8.0 Hz, 1H), 7.95 (t, J = 8.0 Hz, 1H), 7.91 (s, 2H), 7.88 (d, J = 8.0 Hz, 1H), 7.54 (d, J = 2.8 Hz, 1H), 7.49 (dd, J = 8.8, 2.8 Hz, 1H), 4.00 (s, 3H), 3.18 (s, 3H); ^{1}H NMR (400 MHz, $CDCl_3$) δ 8.95 (br s, 1H), 8.62 (br s, 1H), 8.29 (d, J = 8.0 Hz, 1H), 8.18 (d, J = 8.0 Hz, 2H), 7.89 (t, J = 8.0 Hz, 1H), 7.82 (s, 2H), 7.75 (br s, 1H), 7.70 (br s, 1H), 7.38 (s, 1H), 4.02 (s, 3H), 3.38 (s, 3H); ES-MS (ESI+) m/z 329.1 [**15Me**$^+$], 745.2 [**15Me**$^+$]$_2$[BF_4^-]; MS/MS m/z 329 → 314.0 (methyl loss), m/z 745 → 329.1, 314.1, and 270.9.

Model Nitration of Thia-PAHs (For a Typical Procedure, see Supporting Information): 1NO$_2$ (bright yellow solid); yield, 6.4 mg (76% isolate yield); TLC (R_f 0.57, 20% CH_2Cl_2/hexane); mp 197.0−199.0 °C; ^{1}H NMR (500 MHz, $CDCl_3$) δ 8.94 (s, 1H), 8.74 (d, J = 8.5 Hz, 1H), 8.23 (m, 1H), 8.21 (d, J = 8.5 Hz, 1H), 7.97 (m, 1H), 7.77 (t, J = 8.5 Hz, 1H), 7.72 (t, J = 8.5 Hz, 1H), 7.59 (m, 2H); ^{13}C NMR ($CDCl_3$, 125 MHz) δ 144.7 (C),143.9 (C), 139.0 (C), 135.7 (C), 130.4 (C), 129.2 (CH, C), 128.1 (CH), 127.4 (CH), 125.5 (CH), 125.0 (CH), 124.8 (CH), 123.7 (C), 123.1 (CH), 121.8 (CH), 118.5 (CH); IR (KBr) 1533, 1482, 1373, 1143, 1031, 715 cm^{-1}; ES-MS (ESI+) m/z 386.0/387.9 (M + Ag)$^+$.

2NO$_2$ and 2aNO$_2$: The isomeric mixture was isolated after TLC separation (R_f 0.27−0.29, streaks, 20% CH_2Cl_2/hexane) as a bright yellow solid; combined yield, 6.8 mg (73%). **2NO$_2$:** ^{1}H NMR (500 MHz, $CDCl_3$) δ 9.02 (s, 1H), 8.23 (d, J = 7.5 Hz, 1H), 8.13 (d, J = 9 Hz, 1H), 8.22 (d, J = 2.5 Hz, 1H), 7.95 (d, J = 7.5 Hz, 1H), 7.58−7.52 (m, 2H), 7.37 (dd, J = 9.0, 2.5 Hz, 1H), 4.02 (s, 3H); ^{13}C NMR ($CDCl_3$, 125 MHz) δ 127.1 (CH), 126.7 (CH), 125.5 (CH), 123.0 (CH), 121.6 (CH), 120.4 (CH), 119.4 (CH), 103.8 (CH). **2aNO$_2$:** ^{1}H NMR (500 MHz, $CDCl_3$) δ 8.26−8.20 (m, 3H), 7.67 (d, J = 9 Hz, 1H), 7.44 (d, J = 9 Hz, 1H), 7.95 (d, J = 7.5 Hz, 1H), 7.58−7.52 (m, 2H), 4.08 (s, 3H); ^{13}C NMR ($CDCl_3$, 125 MHz) δ 128.2 (CH), 126.7 (CH), 125.0 (CH), 122.9 (CH), 122.9 (CH), 121.7 (CH), 117.8 (CH), 113.5 (CH); ES-MS (ESI+) for **2NO$_2$**/**2aNO$_2$** m/z 415.6/417.6 (M + Ag)$^+$.

3NO$_2$ and 3aNO$_2$: The isomeric mixture was isolated after TLC separation (R_f 0.6, 50% CH_2Cl_2/hexane) as a bright yellow solid; 2.9 mg (38%). **3NO$_2$:** ^{1}H NMR (400 MHz, $CDCl_3$) δ 9.33 (d, J = 8.4 Hz, 1H), 8.67 (d, J = 8.4 Hz, 1H), 8.66 (s, 1H), 8.16 (d, J = 8.0 Hz, 1H), 8.00 (d, J = 8.0 Hz, 1H), 7.94 (t, J = 8.4 Hz, 1H), 7.85 (d, J = 5.2 Hz, 1H), 7.84 (t, J = 8.4 Hz, 1H), 7.68 (d, J = 5.2 Hz, 1H). **3aNO$_2$:** ^{1}H NMR (400 MHz, $CDCl_3$) δ 9.01 (d, J = 8.4 Hz, 1H), 8.44 (s, 1H), 8.08 (d, J = 8.4 Hz, 1H), 8.08 (d, J = 8.4 Hz, 1H), 7.99 (d, J = 8.4 Hz, 1H), 7.99 (d, J = 8.4 Hz, 1H), 7.93 (d, J = 8.4 Hz, 1H), 7.90 (t, J = 8.4 Hz, 1H), 7.77 (d, J = 8.4 Hz, 1H); ES-MS (ESI+) for **3NO$_2$/3aNO$_2$** m/z 386.0/387.9 (M + Ag)$^+$.

4NO$_2$: Isolated as bright yellow solid; yield, 3.6 mg (58%); TLC (R_f 0.33, 40% CH_2Cl_2/hexane); mp 125.0−126.0 °C; ^{1}H NMR (500 MHz, $CDCl_3$) δ 9.30 (d, J = 8.5 Hz, 1H), 8.43 (d, J = 8.5 Hz, 1H), 8.15 (d, J = 9 Hz, 1H), 7.98 (t, J = 8.5 Hz, 1H), 7.83 (t, J = 8.5 Hz, 1H,), 7.76 (d, J = 5 Hz, 1H), 7.71 (d, J = 9 Hz, 1H), 7.65 (d, J = 5 Hz, 1H), 4.16 (s, 3H); ^{13}C NMR (125 MHz, $CDCl_3$) δ 145.1 (C), 139.8 (C), 134.9 (C), 130.9 (C), 129.3 (CH), 127.4 (CH), 127.0 (CH), 126.7, 126.6 (CH), 124.7 (2CH), 124.4 (C), 124.2 (CH), 122.0 (C), 64.0 (CH_3); IR (KBr) 2925, 1522, 1260, 1092, 805 cm^{-1}; ES-MS (ESI+) m/z 416.1/418.0 (M + Ag)$^+$.

5NO$_2$: Isolated as a yellow solid; yield, 3.6 mg (53%); TLC (R_f 0.56, 30% EtOAc/hexane); mp 140.0−142.0 °C; ^{1}H NMR (500 MHz, $CDCl_3$) δ 8.67 (s, 1H), 8.48 (s, 1H), 8.40 (d, J = 8.5 Hz, 1H), 8.20 (d, J = 9.5 Hz, 1H), 8.05 (d, J = 9.5 Hz, 1H), 7.78 (d, J = 5.5 Hz, 1H), 7.68 (d, J = 5.5 Hz, 1H), 7.44 (m, 1H), 4.18 (s, 3H); ^{13}C NMR (125 MHz, $CDCl_3$) δ 132.3 (CH), 126.9 (CH), 124.8 (CH), 124.6 (CH), 124.4 (CH), 120.4 (CH), 118.4 (CH), 126.7 (CH), 107.5 (CH), 55.9 (CH_3) (quaternary carbons not detectable due to very low quantity of this product); IR (KBr) 2964, 1522, 1262, 1099, 803 cm^{-1}; ES-MS (ESI+) m/z 416.0/418.0 (M + Ag)$^+$.

8NO$_2$: Isolated as a yellow solid; yield, 3.1 mg (42%); TLC (R_f 0.27, 15% CH_2Cl_2/hexane); mp 124.0−126.0 °C; ^{1}H NMR (500 MHz, $CDCl_3$) δ 9.15 (d, J = 8.5 Hz, 1H), 8.57 (d, J = 5.5 Hz, 1H), 8.37 (dd, J = 7.0, 1.0 Hz, 1H), 8.15 (d, J = 8.5 Hz, 1H), 7.86 (t, J = 8.5 Hz, 1H), 7.79 (t, J = 8.5 Hz, 1H), 7.82 (d, J = 5.5 Hz, 1H), 7.63 (d, J = 8.5 Hz, 1H), 4.15 (s, 3H); ^{13}C NMR (125 MHz, $CDCl_3$) δ 145.0 (C), 140.6 (C), 134.7 (C), 131.9 (CH), 128.7 (CH), 128.0 (CH), 127.4 (CH), 127.1 (CH), 126.7 (C), 125.2 (CH), 124.6 (C), 123.9 (CH), 123.4 (CH), 121.8 (C), 117.9 (CH), 63.8 (CH_3); IR (KBr) 1528, 1400, 1092, 773, 705 cm^{-1}; ES-MS (ESI+) m/z 416.0/417.9 (M + Ag)$^+$.

11NO$_2$: Isolated as a yellow solid; yield, 6.8 mg (49%); TLC (R_f 0.33, 30% CH_2Cl_2/hexane); mp 193.0−195.0 °C; ^{1}H NMR (500 MHz, $CDCl_3$) δ 9.10 (d, J = 9.5 Hz, 1H), 8.73 (d, J = 8.5 Hz, 1H), 8.02 (d, J = 8.5 Hz, 1H), 8.00 (d, J = 9.0 Hz, 1H), 7.67 (d, J = 9.0 Hz, 1H), 7.62 (t, J = 8.5 Hz, 1H), 7.55 (t, J = 8.5 Hz, 1H), 7.53 (d, J = 9.5 Hz, 1H), 4.09 (s, 3H); ^{13}C NMR (125 MHz, $CDCl_3$) δ 147.3 (C), 140.3 (C), 137.6 (C), 135.8 (C), 128.9 (C), 126.8 (CH), 125.9 (CH), 125.2 (C, CH), 124.5 (2CH), 124.3 (C), 123.5 (CH), 119.5 (CH), 113.4 (CH), 57.0 (CH_3); IR (KBr) 1527, 1358, 1271, 1079, 799 cm^{-1}; ES-MS (ESI+) m/z 416.1/418.1 (M)$^+$.

Model Bromination of Thia-PAHs (For a Typical Procedure, See Supporting Information). 4Br: TLC (R_f 0.56, 40% CH_2Cl_2/hexane); mp 138.0−140.0 °C; ^{1}H NMR (400 MHz, $CDCl_3$) δ 8.95 (d, J = 8.4 Hz, 1H), 8.52 (dd, J = 8.4, 0.8 Hz, 1H), 7.86 (d, J = 8.4 Hz, 1H), 7.85 (m, 1H), 7.77 (d, J = 8.4 Hz, 1H), 7.71 (m, 1H), 7.55 (s, 1H), 7.13 (s, 1H), 4.14 (s, 3H); ^{13}C NMR (125 MHz, $CDCl_3$) δ 153.3 (C), 137.6 (C), 136.0 (C), 131.5 (C), 130.0 (C), 127.6 (CH), 127.0 (CH), 126.9 (C), 126.2 (CH), 125.7 (CH), 125.6 (CH), 122.9 (CH), 122.1 (CH), 121.5 (C), 113.2 (C), 103.2 (CH), 55.6 (CH_3); IR (KBr) 1604, 1253, 1127, 1104, 847 cm^{-1}; ES-MS (ESI+) m/z 449.1/451.0/ 453.0 (M + Ag)$^+$.

6Br and 6Br$_2$: The isomeric mixture was obtained after TLC separation (R_f 0.53, 40% CH_2Cl_2/hexane) as a white solid (3.8 mg, 37% combined isolated yield). **6Br** (major product): ^{1}H NMR (500 MHz, $CDCl_3$) δ 9.20 (d, J = 8.5 Hz, 1H), 8.35 (d, J = 9.0 Hz, 1H), 8.04 (d, J = 8.5 Hz, 1H), 7.98 (d, J = 9.0 Hz, 1H), 7.89 (d, J = 8.5 Hz, 1H), 7.69 (d, J = 5.5 Hz, 1H), 7.61 (d, J = 5.5 Hz, 1H), 7.50 (d, J = 8.5 Hz, 1H), 4.12 (s, 3H); ^{13}C NMR (125 MHz, $CDCl_3$) δ 154.0 (C), 139.8 (C), 134.2 (C), 132.8 (C), 129.9 (CH), 126.6 (CH), 126.3 (CH), 126.1 (CH), 125.3 (C), 124.8 (CH), 124.7 (CH), 122.7 (CH), 121.9 (C), 120.0 (C), 112.1 (CH), 110.7 (C), 56.8 (CH_3). **6Br$_2$** (minor product): ^{1}H NMR (500 MHz, $CDCl_3$) δ 8.87 (d, J = 8.5 Hz, 1H), 8.34 (d, J = 9.0 Hz, 1H), 7.91 (d, J = 9.0 Hz, 1H), 7.88 (d, J = 8.5 Hz, 1H), 7.83 (d, J = 8.5 Hz, 1H), 7.57 (s, 1H), 7.47 (d, J = 8.5 Hz, 1H), 4.11 (s, 3H); ^{13}C NMR (125 MHz, $CDCl_3$) δ 129.8 (CH), 129.4 (CH), 127.3 (CH), 126.6 (CH), 125.0 (CH), 121.6 (CH), 112.1 (CH), 56.7 (CH_3) (quaternary carbons not detectable due to very small quantity of this product); ES-MS (ESI+) m/z 449.1/451.0/452.9 (M + Ag)$^+$.

Acknowledgment. Support of this study under "reactive intermediates of carcinogenesis of PAHs" at KSU by the NCI of NIH (2R15-CA078235-02A1) is gratefully acknowledged.This work was also supported in part by a grant to S.K. (#R826192) by the US-EPA, Washington, D.C.

Supporting Information Available: Experimental and GIAO-derived NMR data and computed changes in NPA-derived charges for various carbocations, representative NMR spectra of the carbocations generated in FSO_3H/SO_2ClF, NMR spectra and specific NMR assignments for the nitro and bromo derivatives, ionization energies for the epoxides, reaction energies for transalkylation, carbocation energies, typical experimental procedures for nitration and bromination, carbocation quenching procedure, computational protocols, stable carbocation generation procedure, and experimental procedures for mutagenicity assays. This material is available free of charge via the Internet at http://pubs.acs.org.

JO701502Y